

Electronic Supplementary Information

Effect of the metal–support interaction in platinum anchoring on heteroatom doped graphene for the enhanced oxygen reduction reaction

*Xin Tong,^{a,b} Xinxing Zhan,^a Zijian Gao,^a Gaixia Zhang,^{*b} Yadian Xie,^c Juan Tian,^a
Hariprasad Ranganathan^b, Dongsheng Li,^d Jerome P. Claverie,^{*e} and Shuhui Sun^{*b}*

a. School of Chemistry and Material Science, Guizhou Normal University, Guiyang, China, 55000.

b. Institut National de la Recherche Scientifique (INRS)-Centre Énergie Matériaux Télécommunications, Varennes, QC, J3X 1P7 Canada.

c. Key Laboratory of Low-Dimensional Materials and Big data, Guizhou Minzu University, Guiyang 550025, China.

d. College of Materials and Chemical Engineering, Key Laboratory of Inorganic Nonmetallic Crystalline and Energy Conversion Materials, China Three Gorges University, Yichang, 443002 P. R. China.

e. Department of Chemistry, Université de Sherbrooke, Sherbrooke, QC, J1K 2R1 Canada.

Corresponding authors: gaixia.zhang@inrs.ca (G. Zhang);
Jerome.Claverie@USherbrooke.ca (J. Claverie); shuhui.sun@inrs.ca (S. Sun)

1. Experimental Section

1.1 Doping heteroatoms into graphene

All the chemicals are purchased from Sigma-Aldrich Company unless specified. GO was synthesized by an improved Hummers' method using natural graphite flake (325 mesh, metal basis). For N, P-graphene, GO was dispersed in DI water, followed by the addition of triphenylphosphine (Ph_3P) ether solution in a weight ratio of 1:5. Then the mixture was ultra-sonicated for 4h and stirred for another 4 h at room temperature. This precursor solution was vacuum dried at 60°C for at least 24 h. Subsequently, the powders were heated at 200 °C for 1 h under an argon atmosphere, and then the temperature was raised to 950 °C and kept for 15min while feeding Ar (100 sccm) and NH_3 (100 sccm) at room pressure. The preparation of N-Graphene follows similar procedures, without the Ph_3P mixing process. For RGO, a similar annealing process was achieved under an inert argon atmosphere.

1.2 Loading the Pt Catalyst on graphene Materials

Pt catalysts were loaded on graphene materials (i.e., RGO, N-Graphene, and N, P-Graphene) by the traditional wet impregnation method. First, graphene material was added into water and sonicated for 2h, followed by adding an aqueous $\text{H}_2\text{PtCl}_6 \cdot 6\text{H}_2\text{O}$ solution in a weight ratio of 1:20. After 2 hours of violent magnetic stirring, the products were washed with water and freeze-dried for 12h. Then, the mild heat treatment of the powder was performed at 450°C for 2 h under an inert argon atmosphere with a flow rate of 100 mL min^{-1} .

1.3 Physical Characterizations.

The morphology of all catalysts was characterized by a JEM-2200FS transmission electron microscope (TEM) operated at 200 kV. To estimate the particle size of Pt, 100 particles were selected randomly in the TEM images and measured by the ImageJ software.¹ The scanning electron microscope (SEM) images and energy dispersive spectroscopy (EDS) were achieved by Tescan Vega3 LMH. Inductively Coupled Plasma/Optical emission spectrometry (ICP-OES, Agilent Technologie, 5100) was used to analyze the Pt contents. Chemical analysis of the surface was characterized by X-ray photoelectron spectroscopy (XPS) with a VG Escalab 220i-XL using Mg K α line as an excitation source. The X-ray diffraction (XRD) patterns were recorded with Rigaku D/max 2550VB. The Raman spectra was collected on a Jobin-Yvon Labram-1b with 632.8nm laser excitation.

1.4 Electrochemical Characterizations.

Electrochemical measurements were performed in a three-electrode cell with a bipotentiostat (Pine, Model PGSTAT-72637) workstation at room temperature. A Pt wire was used as the counter electrode, and a saturated calomel electrode (SCE) was served as the reference electrode, which was calibrated by a reversible hydrogen electrode (RHE) before the test. The rotating ring-disk electrode (RRDE) (0.252 cm², PINE Instrumentation) was used as the working electrode. The commercial 20% Pt/C were purchased from TKK company (TKK TEC10E20A). The catalyst ink is prepared as follows, 5 mg of catalyst was mixed in a glass vial with 1650 μ l of ethanol, 85 μ l of water, 47.5 μ l of 5 wt.% Nafion solution, and five small glass beads, followed by sonication and agitation in a vortex mixer, alternatively, for three times. Then 18 μ l of

the catalyst suspension was dropped onto the GC electrode surface of RRDE (with the loading of $\sim 10 \mu\text{g Pt cm}^{-2}$). Before the electrochemical tests, the cycling voltammograms (CVs) between 0.03 and 1.20 V (vs. RHE) at 200 mV/s for 50 cycles were run in an N_2 -saturated 0.1 M HClO_4 to activate the electrocatalyst. The linear sweep voltammograms (LSV) were recorded at 10 mV s^{-1} , between 0.03-1.2 V (vs. RHE). The chronoamperometric (CA) measurement was achieved at a constant potential of 0.8v versus RHE using the carbon rod as a counter electrode. The kinetic currents were calculated using the Koutecky–Levich equation:

$$\frac{1}{J} = \frac{1}{J_k} + \frac{1}{J_L} \quad (1)$$

Where J , J_k , and J_L represent the measured, kinetic and diffusion-limited (Levich) current densities, respectively.

The peroxide yield ($\text{H}_2\text{O}_2\%$) and the electron transfer number (n) were calculated as equation (2) - (3):

$$\text{H}_2\text{O}_2\% = \frac{200I_R/N}{(I_R/N + I_D)} \quad (2)$$

$$n = \frac{4I_D}{(I_R/N + I_D)} \quad (3)$$

Where I_D is the disk current, I_R is the ring current, and N is the collection efficiency, equal to 0.37 for the present case.

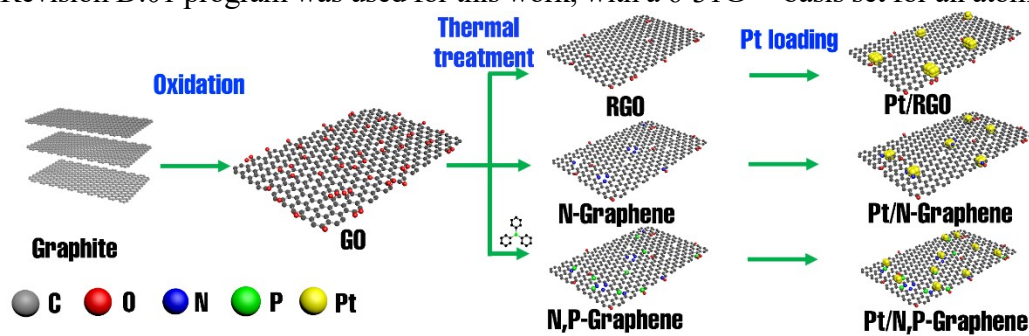
The following equation was used to calculate the ECSA of Pt:

$$\text{ECSA} = \frac{Q_H}{M_{\text{Pt}}q_H} \quad (4)$$

where Q_H is the charge for hydrogen adsorption region in CV, m_{Pt} is the loding of Pt, and q_H is constant ($0.21 \text{ mC}\cdot\text{cm}^{-2}$, when the hydrogen is monolayer adsorbed on Pt surface).

1.5 Computational Details

The B3LYP-D3 (BJ) hybrid density functional theory (DFT) in the GAUSSIAN 16, Revision D.01 program was used for this work, with a 6-31G** basis set for all atoms. ²



Scheme S1. Schematic illustration of the fabrication process of Pt supported on RGO, N-graphene and N,P-graphene.

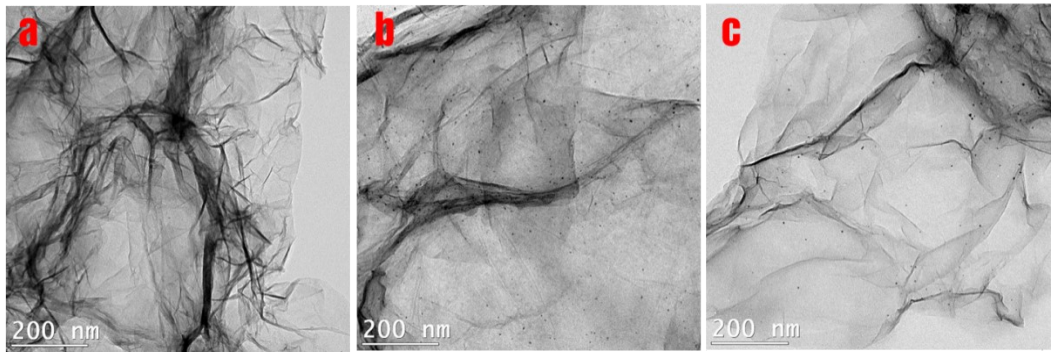


Figure S1. Low magnification TEM images of (a) Pt/N, P-Graphene, (b) Pt/N-Graphene and (c) Pt/RGO.

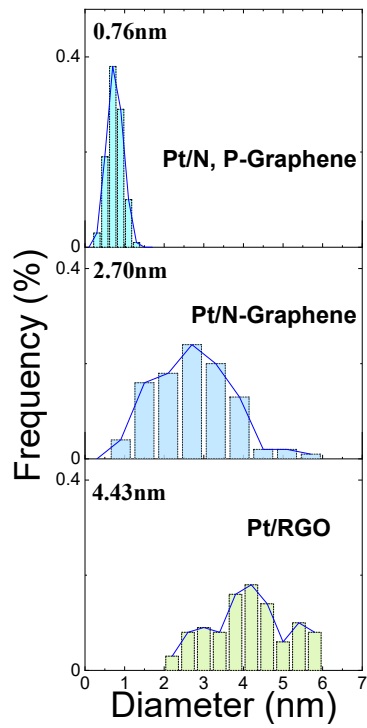


Figure S2. The size-distribution histogram of Pt/N, P-Graphene, Pt/N-Graphene and Pt/RGO.

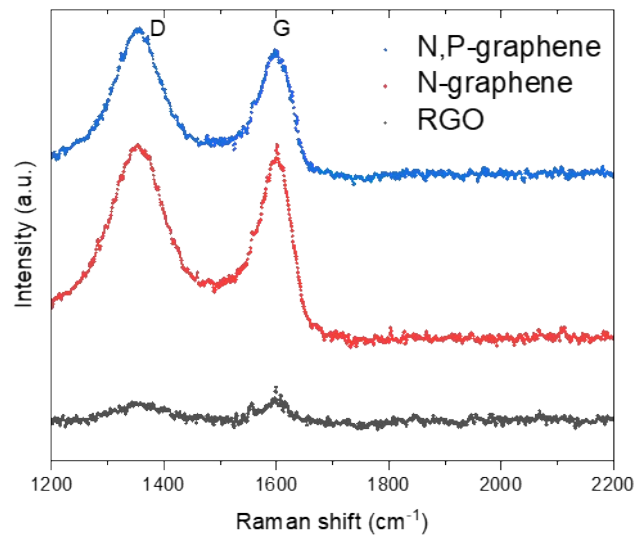


Figure S3. Raman spectra of RGO, N-Graphene, and N,P-Graphene.

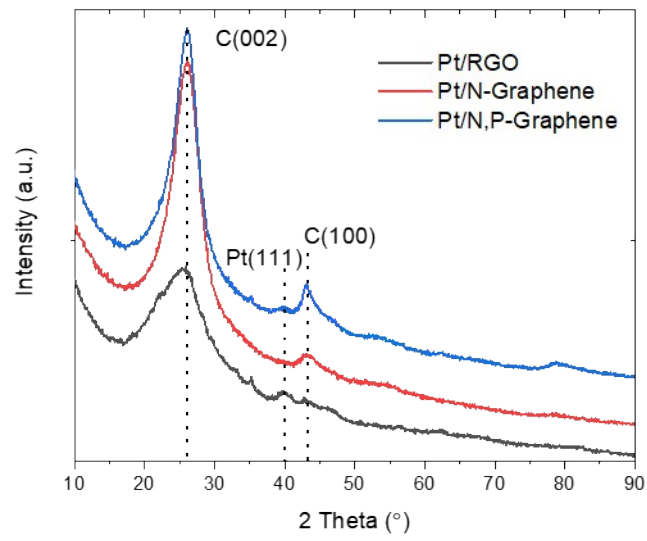
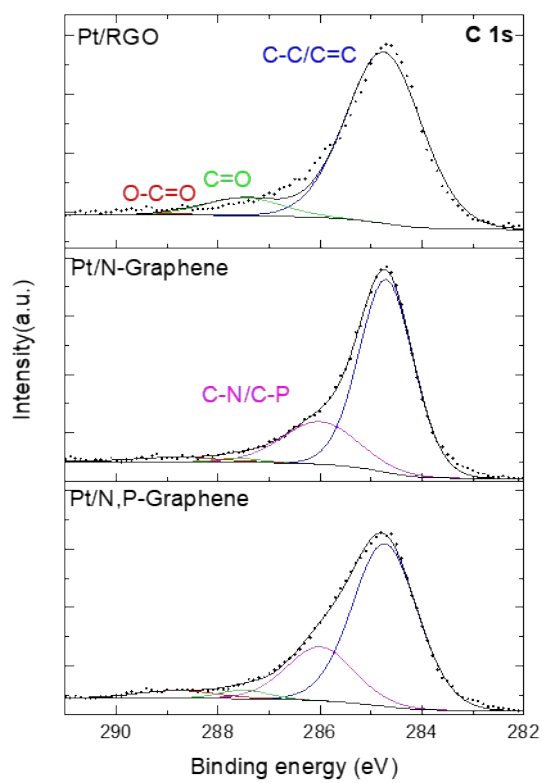
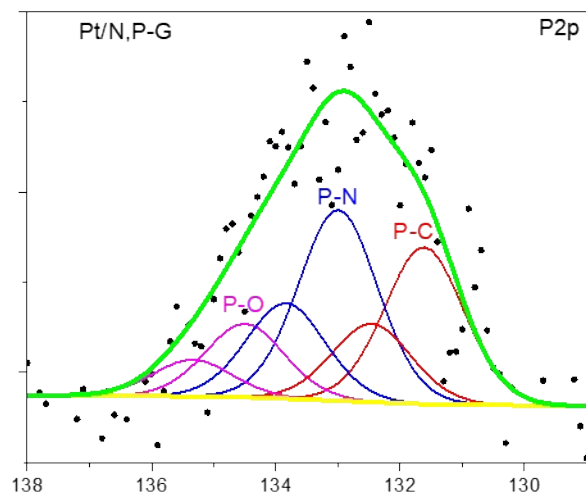


Figure S4. XRD patterns of Pt/N,P-Graphene, Pt/N-Graphene, and Pt/RGO.



FigureS5. High-resolution XPS spectra of C1s of Pt/RGO, Pt/N-Graphene, and Pt/N,P-Graphene.



FigureS6. High-resolution XPS spectra of P2P of Pt/N, P-Graphene.

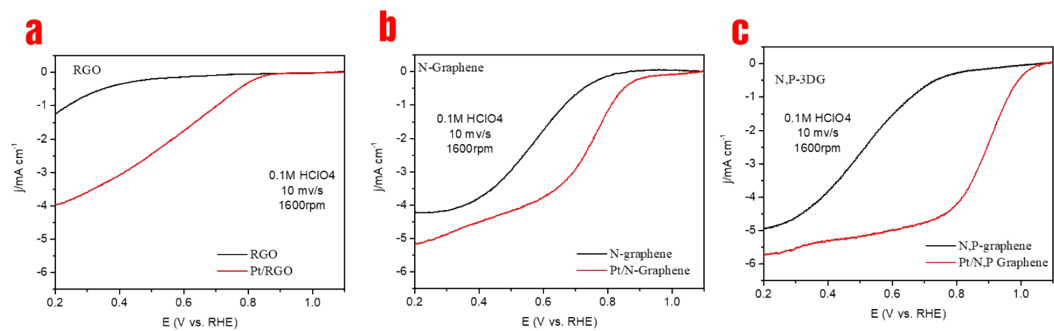


Figure S7. (a,b,c) LSV on RRDE of RGO and Pt/RGO, N-Graphene and Pt/N-Graphene, N,P-Graphene and Pt/N,P-Graphene in O_2 -saturated 0.1 M HClO_4 at a scan rate of 10 mV s^{-1} (rotation speed: 1600 rpm).

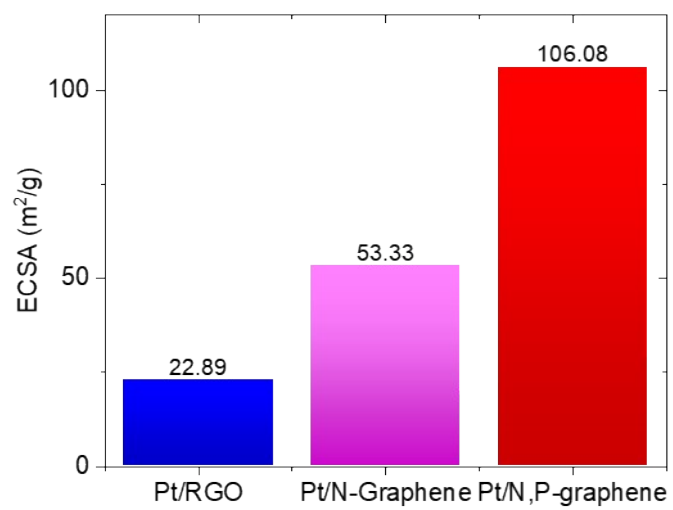


Figure S8. The ECSA of Pt/RGO, Pt/N-Graphene, and Pt/N,P-Graphene.

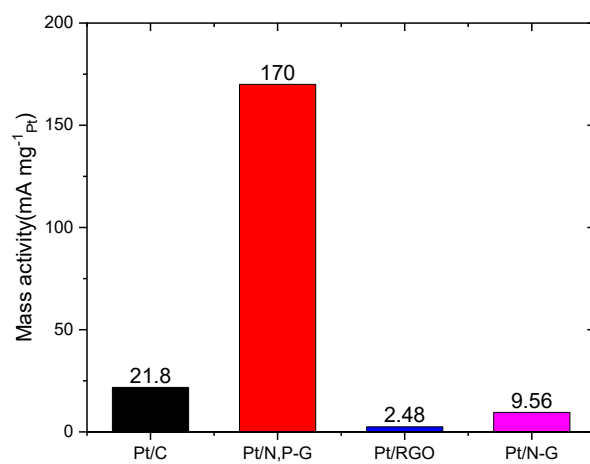


Figure S9. The mass activity of these four catalysts was normalized by the weight of Pt at 0.9 V versus RHE.

Table S.1 Elemental quantification of Pt/N, P-Graphene, Pt/N-Graphene, and Pt/RGO obtained from XPS results.

Sample	C Element content /at. %	O Element content /at. %	N Element content /at. %	P Element content /at. %	Pt ^a Element content /at. %
Pt/RGO	82.65	12.47	-	-	4.88
Pt/N- Graphene	85.27	6.39	3.13	-	5.03
Pt/N,P- Graphene	87.36	3.18	3.31	0.93	5.22

^{a)} Pt contents were analyzed by ICP-OES.

Table S.2 Curve fitting results of the XPS N1s spectrum.

Sample	Peak assign									
	Pyridinic-N		Pyrolic-N		N-P		Graphitic-N		N-oxide	
	BE(eV)	%	BE(eV)	%	BE(eV)	%	BE(eV)	%	BE(eV)	%
Pt/N-Graphene	398.1	36.63	399.5	29.12	-	-	401.4	31.86	403.5	2.39
Pt/N,P-Graphene	398.1	32.05	399.5	27.50	400.8	22.04	401.5	15.68	403.5	2.73

Table S3. Summary of some typical work on ORR.

The Catalyst	Supports	Synthesis method	Pt content	Half-wave Potential	ECSA (m ² /g)	Ref.
Pt/N, P-Graphene	N, P-Graphene	Annealing and wet impregnation method	5.22 wt%	0.88 V vsRHE	106	Our work
Pt/(Mn-N)@C	Mn-Nx composite	Calcination-chemical reduction	17.6 wt%	0.928 V vsRHE	76.6	3
PtNPC	N,P-doped carbon hollow spheres	Two-step impregnation-calcination method	0.026 wt%	0.85V vsRHE in 0.1M KOH	-	4
Pt/CNF-1300-0.28Mn	Mn-modified polyaniline-based carbon nanofibers	Pyrolysis - chemical reduction	20 wt%	0.891 V vsRHE	-	5
Pt@NPC	N,P-doped carbon	SiO ₂ templates based pyrolysis method	2.2 wt %	0.872 V vsRHE	83.89	6
Pt/NCWG	Conductive nanocarbon wedged N-doped graphene	Lyophilization assisted N-doping method	20 wt %	~0.85 V vsRHE	96.4	7
Pt/BP defect	Defeat carbon	Annealing method	1.1 wt%	0.85 V vsRHE	-	8
Pt-ON/C	Co _{0.4} Mo _{0.5} O _x N _y	Annealing method	2 wt%	0.76 V vsRHE	-	9
Pt-N/BP	Pyridinic-N doped carbon	Annealing method	0.4 wt %	0.76 V vsRHE	-	10
Pt/NH ₂ -graphene	Graphene with surface Functionalization	Chemical method	30 wt%	~0.85 V vsRHE	59.3	11
d-FeN ₄	micropores carbon	pyrolysis method	-	0.83 V vsRHE	-	12

Reference

1. J. Schindelin, I. Arganda-Carreras, E. Frise, V. Kaynig, M. Longair, T. Pietzsch, S. Preibisch, C. Rueden, S. Saalfeld, B. Schmid, J.-Y. Tinevez, D. J. White, V. Hartenstein, K. Eliceiri, P. Tomancak and A. Cardona, *Nat Methods*, 2012, **9**, 676-682.
2. M. Frisch, G. Trucks, H. B. Schlegel, G. E. Scuseria, M. A. Robb, J. R. Cheeseman, G. Scalmani, V. Barone, B. Mennucci and G. Petersson, *Inc., Wallingford CT*, 2009, **201**.
3. Q. Shu, J. Zhang, B. Hu, X. Deng, J. Yuan, R. Ran, W. Zhou and Z. Shao, *Energ Fuel*, 2022, **36**, 1707-1715.
4. X. Zhu, X. Tan, K.-H. Wu, S.-C. Haw, C.-W. Pao, B.-J. Su, J. Jiang, S. C. Smith, J.-M. Chen, R. Amal and X. Lu, *Angewandte Chemie International Edition*, 2021, **60**, 21911-21917.
5. J. Yu, Q. Zhou, X. Xue, H. Zhang, X. Li, F. Wang, Q. Chen and H. Zhu, *New J Chem*, 2021, **45**, 14608-14615.
6. W. Tian, Y. Wang, W. Fu, J. Su, H. Zhang and Y. Wang, *J Mater Chem A*, 2020, **8**, 20463-20473.
7. Y. Xiong, M. You, F. Liu, M. Wu, C. Cai, L. Ding, C. Zhou, M. Hu, W. Deng and S. Wang, *ACS Applied Energy Materials*, 2020, **3**, 2490-2495.
8. J. Liu, M. Jiao, B. Mei, Y. Tong, Y. Li, M. Ruan, P. Song, G. Sun, L. Jiang, Y. Wang, Z. Jiang, L. Gu, Z. Zhou and W. Xu, *Angew Chem Int Ed Engl*, 2019, **58**, 1163-1167.
9. L. Wang, P. Wurster, P. Gazdzicki, M. Roussel, D. G. Sanchez, L. Guetaz, P. A. Jacques, A. S. Gago and K. A. Friedrich, *J Electroanal Chem*, 2018, **819**, 312-321.
10. J. Liu, M. Jiao, L. Lu, H. M. Barkholtz, Y. Li, Y. Wang, L. Jiang, Z. Wu, D.-j. Liu, L. Zhuang, C. Ma, J. Zeng, B. Zhang, D. Su, P. Song, W. Xing, W. Xu, Y. Wang, Z. Jiang and G. Sun, *Nat Commun*, 2017, **8**, 15938.
11. L. Xin, F. Yang, S. Rasouli, Y. Qiu, Z.-F. Li, A. Uzunoglu, C.-J. Sun, Y. Liu, P. Ferreira, W. Li, Y. Ren, L. A. Stanciu and J. Xie, *Acs Catal*, 2016, **6**, 2642-2653.
12. Z. Li, R. Ma, Q. Ju, Q. Liu, L. Liu, Y. Zhu, M. Yang and J. Wang, *The Innovation*, 2022, **3**, 100268.